

A fast and comprehensive microdisc laser model applied to all-optical wavelength conversion

J. Hofrichter¹, O. Raz², F. Horst¹, N. Chrysos¹, C. Minkenberg¹, T. de Vries², H.J.S. Dorren², R. Kumar³, L. Liu³ and B.J. Offrein¹

1: IBM Research GmbH, IBM Research – Zurich, Säumerstrasse 4, 8803 Rüschlikon, Switzerland

2: COBRA Research Institute, Eindhoven University of Technology, P.O. Box 512, 5600MB Eindhoven, The Netherlands

3: Photonics Research Group, INTEC Department, Ghent University – IMEC, St. Pietersnieuwstraat 41, 9000 Ghent, Belgium

Abstract: Microdisc lasers (MDLs) are an attractive option for on-chip laser sources, wavelength converters and even all-optical optical memory. We have developed a comprehensive model for the wavelength conversion in MDLs, which is compared with measurements.

©2010 Optical Society of America

OCIS codes: (130.7405) Wavelength conversion devices; (230.7405) Wavelength conversion devices

1. Introduction

Microdisc lasers (MDLs) heterogeneously integrated on silicon wafers [1] as shown in Figs. 1(a) and (b) are an interesting candidate for on-chip laser sources [2], all-optical wavelength converters [3,4] and also all-optical memories [5,6]. Here, we investigate MDLs to demonstrate all-optical signal processing and switching. Within a MDL, several modes are competing. Several longitudinal modes may lase simultaneously, originating from the free spectral range (FSR) of the cavity being smaller than the broad gain spectrum of the MQW gain material. All these modes may lase in both the clockwise and the counter-clockwise direction. Typically several lasing peaks are present as indicated in Fig. 1(c), where the main lasing mode is located at approx. 1585 nm, and the higher wavelength side-mode is present at approx. 1617 nm.

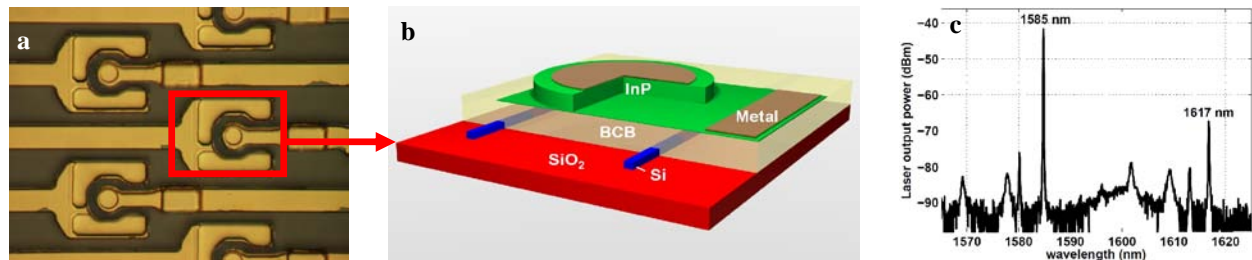


Fig. 1 – A MDL on a SOI waveguide, (a) microscope image, (b) cross section, (c) typical lasing spectrum of a MDL

Earlier numerical models of MDLs have concentrated on the dynamics of two counter propagating modes at the same wavelength [7,8]. These models cannot simulate the competition between longitudinal modes in gain-dispersive media. There exists a model to describe the latter, using an estimated parabolic dependency of the gain with wavelength [9]. In this work, we have combined these models into a single model, simulating a disc laser having several co- and counter propagating modes. In the next section, the model will be described and in section 3, simulation results will be compared with measurements [4].

2. The 1D microdisc laser model

To accurately simulate the behavior of a MDL as a wavelength converter, we implemented a 1D laser rate equation model. We expanded the model suggested by Van Campenhout *et al.* [1] for several modes and included self and cross gain suppression with the corresponding factors ε_S and ε_C [7-9]. A parabolic gain curvature was assumed to account for the non-uniform gain spectrum [10]. Equation (1) gives the radially dependent gain term where G_0 is the maximum gain at the central lasing mode λ_0 and a is the gain curvature parameter. To save computation time and speed up the model, the photon densities $S_{cw,ccw,i}$ are modelled as lumped photon densities of the i -th mode with the corresponding propagation direction. Because we have a quantum well active material for the given devices, logarithmic gain is assumed, where N_0 is the threshold carrier density.

$$g_{cw,ccw}(S_{cw}, S_{ccw}, n(r), r) = G_0 \left[1 - a(\lambda_0 - \lambda)^2 \right] \cdot (1 - \varepsilon_S \sum_i S_{cw,ccw,i} - \varepsilon_C \sum_i S_{ccw,cw,i}) \cdot \ln \frac{n(r)}{N_0} \quad (1)$$

In Eq. (2), the carrier density is locally reduced by stimulated emission into the corresponding mode. Therefore the overlap with the modal distribution $\Psi(r)$ is being calculated. For whispering gallery cavities, $\Psi(r)$ can be approximated by a normalized Bessel function of the first kind $J_\nu(r/z_0)$, where ν is the azimuthal order of the

corresponding mode and z_0 the first Bessel zero of $J_\nu(z)$. The modal distribution is normalized such that

$$\int_0^R \Psi^2(r) r dr = 1.$$

$$\frac{\partial n(r)}{\partial t} = - \left[\sum_i g_{CW,i}(r) S_{CW,i} + \sum_i g_{CCW,i}(r) S_{CCW,i} \right] v_g \Psi^2(r) \Gamma \pi R^2 - An(r) - Bn(r)^2 - Cn(r)^3 + \frac{\eta I}{\pi R^2 q t_a} + D \left(\frac{\partial n(r)}{\partial r} + \frac{\partial^2 n(r)}{r \partial r^2} \right) \quad (2)$$

Besides stimulated emission into the respective lasing modes, also non-lasing recombination is taken into account by the coefficients A , B and C for one, two and three particle processes, respectively. The electrical pumping current I flowing through the disk area πR^2 generates charge carriers in the active region, whose thickness is t_a . Regions with depleted carrier concentrations due to stimulated emission in the region of the mode (spatial hole-burning) are refilled by diffusion of charge carriers with the diffusion constant D . In contrast to Eqs. (1) and (2) the photon densities defined in Eq. (3) are modelled by lumped variables whose spatial distribution is obtained from $\Psi(r)$. Each photon density experiences a decay time constant τ_p due to e.g. scattering or absorption.

$$\begin{aligned} \frac{\partial S_{CW,CCW,i}}{\partial t} = & - \frac{S_{CW,CCW,i}}{\tau_p} + S_{CW,CCW,i} \Gamma v_g 2\pi \int_0^R g_{CW,CCW,i}(r) \Psi^2(r) r dr + 2\pi \beta \int_0^R Bn^2(r) \Psi^2(r) r dr \\ & + k_{int} S_{CCW,CW,i} + k_{ext} \sqrt{S_{ext,CW,CCW,i} S_{CW,CCW,i}} \end{aligned} \quad (3)$$

The build-up of the mode is achieved by stimulated emission with the modal gain $g_{CW,CCW,i}$ in the active region, whose overlap with the mode is Γ . Also spontaneous emission with the factor B is coupled into the lasing mode with the spontaneous emission coupling factor β . In addition, scattering due to sidewall roughness causes a coupling of the counter-propagating modes which is modelled by k_{int} [11]. The external injection coupling factor k_{ext} models the coherent external injection [7,8] of light into the respective lasing mode. Table I lists the values of the parameters used in the model. The model's radial dependency enables the simulation of spatial hole-burning which limits output power, modal recovery and thus the device speed.

Table I. Simulation parameters

Param.	R	G_0	N_0	ϵ_s	ϵ_c	k_{int}	k_{ext}	v_g	λ_0
Value	3.75 μm	1500 cm^{-1}	1.5e18 cm^{-3}	2e-17 cm^3	4e-17 cm^3	1.5e8 s^{-1}	8.8e10 s^{-1}	8.817e9 cm s^{-1}	1550 nm
Param.	A	B	C	D	β	η	I	a	t_a
Value	1e-8 s^{-1}	2e-10 $\text{cm}^3 \text{s}^{-1}$	1.63e-28 $\text{cm}^6 \text{s}^{-1}$	8 $\text{cm}^2 \text{s}^{-1}$	1e-3	0.267	3 mA	1.3e13 cm^{-3}	18 nm

3. Simulations and experiments

MDLs can be operated as wavelength converters by injecting light into the non-dominant lasing mode, i.e., the mode at approx. 1617 nm in Fig. 1(c) for our case. By gain suppression, the previously dominant central lasing mode i.e. the mode at approx. 1586 nm, is suppressed. In order to operate at high bit rates and high repetition rates, we accelerated the recovery of the central by seeding low-power continuous-wave light into the central lasing mode [3,4]. When monitoring the relative eye opening $EO = (P_{1,eye} - P_{0,eye}) / P_{1,max}$ during wavelength conversion, it becomes clear that seeding improves the eye opening for both 10 Gb/s and 20 Gb/s, As can be seen from Figs. 3(a) and (b), the EO is strongly improved by seeding of continuous-wave light into the central mode.

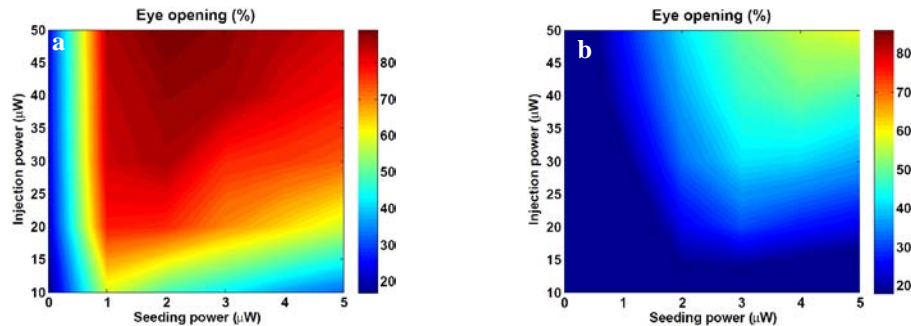


Fig. 3 – Relative eye opening (EO) in % at (a) 10 Gb/s and (b) 20 Gb/s.

The eye diagram for 50 μW signal injection in the absence of seeding is reproduced in Figs. 4(a) and (d) for 10 and 20 Gb/s. The largest EOs that can be achieved with seeding are shown in Figs. 4(b) and (e) for 10 and 20 Gb/s, respectively. The simulated eye diagrams demonstrate excellent agreement with the experimental data in Figs. 4(c)

and (f). Although the power levels in the waveguide are experimentally inaccessible, the rise and fall times are not only equivalent but also symmetric in both cases. From Fig. 4(b) the 10%-to-90% rise time was estimated to be approx. 55 ps. To further improve the operation speed of the devices, a higher external signal injection may be used. It was also found that a lower total intensity in the cavity, i.e. a smaller disc diameter, leads to faster switching time. Experimentally [4], the scheme of injection seeded disc lasers wavelength converter was shown to operate error-free with a bit-error rate (BER) of below 10^{-9} for the operation at 10 Gb/s when using seeding. Although the eye for 20 Gb/s looks degraded, a BER of below 10^{-3} was achieved which is still below the forward-error correction (FEC) limit and thus acceptable for some applications.

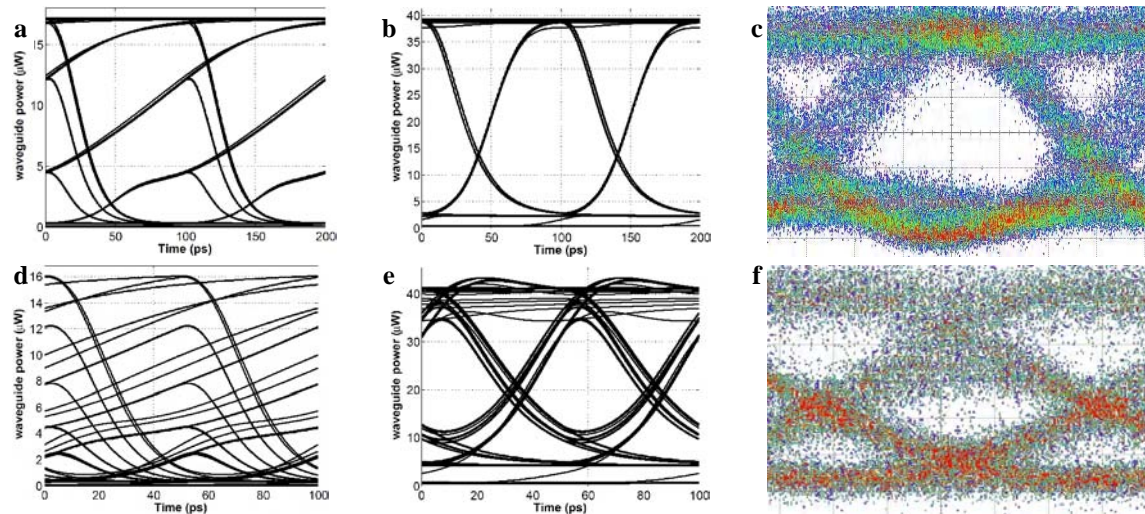


Fig. 4 – Wavelength conversion: Simulation at 10 Gb/s with 50 μ W injection and (a) without seeding, (b) with 2 μ W seeding, (c) measurement at 10 Gb/s with seeding. Simulation at 20 Gb/s with 50 μ W injection and (d) without seeding, (e) with 5 μ W seeding, (f) measurement at 20 Gb/s with seeding.

4. Conclusion

We have presented a fast and comprehensive model for the simulation of MDLs. The numerical studies on wavelength conversion of MDLs provided excellent agreement with measurements at both 10 and 20 Gb/s. It was shown that with seeding, wavelength conversion can be performed at 20 Gb/s with an acceptable BER. The model holds promise to facilitate the further exploration of various MDL functionalities, and to guide experimental work.

5. Acknowledgment

The authors acknowledge the financial support by the European Union FP7-ICT project “HISTORIC”.

- [1] J. v. Campenhout, P. Rojo-Remeo, P. Regreny, C. Seassal, D. v. Thourhout, S. Verstuyft, L. Di Cioccio, J.-M. Fedeli, C. Lagahe and R. Baets, “Electrically pumped InP-based microdisk lasers integrated with a nanophotonic silicon-on-insulator waveguide circuit,” *Opt. Express* **15**(11), 6744–6749 (2007).
- [2] L. Liu, J. v. Campenhout, P. Rojo-Romeo, P. Regreny, C. Seassal, D. v. Thourhout, S. Verstuyft, L. Di Cioccio, J.-M. Fedeli, C. Lagahe and R. Baets, “Compact multiwavelength laser source based on cascaded InP-microdisks coupled to one SOI waveguide,” in *OSA Technical Digest “Optical Fiber Communication Conf. and Exposition and The National Fiber Optic Engineers Conf.”* (OSA, 2008), paper OWQ3.
- [3] O. Raz, “High speed wavelength conversion in a heterogeneously integrated disc laser over silicon on insulator for network on a chip applications,” *Proc. ECOC*, Vienna, Austria, 2009.
- [4] O. Raz, “Compact, Low power and low threshold electrically pumped micro disk lasers for 20Gb/s non return to zero all optical wavelength conversion,” to be presented at *OFC 2010*, San Diego, CA, USA, paper OMQ5.
- [5] M.T. Hill, “A fast low-power optical memory based on coupled micro-ring lasers,” *Nature* **432**, 206-209 (2004).
- [6] L. Liu, R. Kumar, K. Huybrechts, T. Spuesens, G. Roelkens, E.-J. Geluk, T. d. Vries, P. Regreny, D. v. Thourhout, R. Baets and G. Morthier, “An ultra-small, low-power, all-optical flip-flop memory on a silicon chip,” *Nature Photonics* **268**, 1-6 (2010).
- [7] C.L. Tang, A. Schremer and T. Fujita, “Bistability in two-mode semiconductor lasers via gain saturation,” *Appl. Phys. Lett.* **51**(18), 1392-1394 (1987).
- [8] G. Yuan and S. Yu, “Bistability and switching properties of semiconductor ring lasers with external optical injection,” *IEEE J. Quantum Electron.* **44**(1), 41-48, 2008.
- [9] M.J. Adams and M. Osihski, “Longitudinal mode competition in semiconductor lasers: Rate equations revisited,” *IEE Proc., Part I: Solid State Electron Devices* **129**(6), 271-274 (1982).
- [10] W.E. Lamb, Jr., “Theory of an optical maser,” *Phys. Rev. A* **134**, 1429-1450 (1964).
- [11] R. Kumar, L. Liu, G. Roelkens, G. Morthier and R. Baets, “Simple and accurate measurements to characterize microdisk lasers for all-optical flip-flop operation,” *Proc. Ann. Symp. IEEE Photonics Benelux Chapt., Belgium* (2009).